

# Research

# Long-term mechanistic hindcasts predict the structure of experimentally-warmed intertidal communities

Diana E. LaScala-Gruenewald and Mark W. Denny

D. E. LaScala-Gruenewald (https://orcid.org/0000-0001-9635-6260) ☑ (dianalg@mbari.org) and M. W. Denny, Dept of Biology, Stanford Univ., Stanford, CA 94305, USA. Present address for DELG: Monterey Bay Aquarium Res. Inst., Moss Landing, CA 95039, USA.

Oikos 129: 1645–1656, 2020

doi: 10.1111/oik.07468

Subject Editor: Morgan Kelly Editor-in-Chief: Dries Bonte Accepted 30 June 2020 Increases in global temperatures are expected to have dramatic effects on the abundance and distribution of species in the coming years. Intertidal organisms, which already experience temperatures at or beyond their thermal limits, provide a model system in which to investigate these effects. We took advantage of a previous study in which experimental plates were deployed in the intertidal zone and passively warmed for 12 years to a daily maximum temperature on average 2.7°C higher than control plots on the adjacent bedrock. We compared the composition of the biological communities on each experimental plate with its neighboring bedrock control. Plate communities showed decreased richness of taxa and percent cover of filamentous algae, mussels and mobile grazers relative to bedrock, and increased percent cover of biofilm. We then used short-term time-series measurements of plate and bedrock temperatures and a mechanistic heat-budget model to hindcast those temperatures back 12 years. Greater differences in long-term average temperature between the experimental plates and bedrock controls were correlated with lower similarity in community composition. Additionally, years with higher average differences between plate and bedrock temperatures were more predictive of current compositional similarity between plate and bedrock communities, even though they occurred farther in the past than did more recent, but cooler, years. We conclude that current intertidal communities reflect their long-term, rather than short-term, thermal histories. Mechanistic heat-budget models based on short-term measurements can provide this valuable, long-term information.

Keywords: climate change, community structure, field-based experimental warming, heat-budget model, intertidal zone

### Introduction

Global average air temperature is expected to rise between 1.0 and 3.7°C by the end of this century (Pachauri and Meyer 2014) with potential effects on biological communities worldwide. Paleoclimatic records show that similar changes in temperature can result in shifts in the distribution or abundance of species (Kennett and Stott 1991), and, already, poleward shifts in modern species distributions have been observed (Parmesan 2006, Hawkins et al. 2008). Shifts in demography (Parmesan and Yohe 2003), population-level size distributions (Gardner et al. 2011, Sheridan and Bickford



www.oikosjournal.org

© 2020 Nordic Society Oikos. Published by John Wiley & Sons Ltd

2011) and species richness (Gruner et al. 2017) have been recorded. However, within broad latitudinal gradients, regional hot and cool spots may mitigate the effects of climate change (Helmuth et al. 2002, 2006a). Warming is also likely to have differential non-lethal impacts on organisms, affecting energetics and behavior, and ultimately the strength of ecological interactions and community structure and dynamics (Graham and Grimm 1990, Fields et al. 1993, Sanford 1999, Harley 2011). These issues complicate the analysis of climatic effects.

Thus far, evidence for community-level shifts due to climate warming has been based largely on correlations between natural temperature increases and changes in species' distributions or abundances (Sagarin et al. 1999, Helmuth et al. 2006b, Blenckner et al. 2007), comparisons between communities across latitudinal gradients (Bertness et al. 1999), and ecological forecasts using heat-budget and climate envelope (environmental niche) models (Davis et al. 1998, Helmuth 1998). The first two methods typically lack an experimental control that could demonstrate a causal link between community-level shifts and temperature changes, while modeling approaches are sensitive to assumptions, and often rely on a single physical predictor (Helmuth et al. 2006b). To be of greatest value, observational and modeling approaches must be applied in concert with in situ, controlled experiments that test for mechanistic links between temperature changes and community composition (Shaver et al. 2000).

The wave-swept, rocky intertidal zone has long been a model system for experimental ecology, and is ideal for performing manipulative, in situ experiments that explore the effects of climate change. Because intertidal organisms are relatively small and their movement is often limited, manipulative, in situ experiments are tractable (Kordas et al. 2015). In addition, rocky intertidal communities may serve as early warning systems for climate change (Barry et al. 1995, Thompson et al. 2002, Harley et al. 2006, Helmuth et al. 2006a). Because intertidal organisms must endure terrestrial conditions during low tides, they may episodically experience body temperatures at or above their thermal limits (Hofmann and Somero 1995, Davenport and Davenport 2005). Consequently, dramatic shifts in community composition, vertical species distributions and community dynamics are likely to be observed in conjunction with even small increases in aerial temperature (Somero 2002, Harley et al. 2006, Denny et al. 2009).

Despite the relevance and relative tractability of manipulative experiments in the intertidal zone, few studies have examined the effects of warming on community structure (Schiel et al. 2004, Kordas et al. 2015, Dal Bello et al. 2017). Kordas et al. (2015) used settlement plates warmed in situ on the coast of British Columbia to test the short-term effects of increased temperature on intertidal communities. Many intertidal organisms have body temperatures that are primarily determined by substrate temperature (Denny and Harley 2006), and substrate warming is therefore a close proxy to increased aerial temperatures (Denny et al. 2006, Kordas et al. 2015). Using this experimental strategy,

Kordas et al. were able to increase the average maximum daily temperatures experienced by the communities by 1.5–2.9°C for a year. They found that barnacles and gastropod grazers fared poorly, but that filamentous algae were unaffected.

To our knowledge, Kordas et al. (2015) represents the first study to examine the effects of climate change on intertidal communities through direct, in situ experimentation. However, because the impacts of warming are expected to be strongly modulated by local environmental and biological factors (Helmuth et al. 2006a) more experimentation is needed. In addition, Kordas et al. (2015) tracked temperatures and communities in the intertidal zone between April 2009 and March 2010. This allowed them to observe the settlement, survival and phenology of intertidal organisms across seasons, but did not address the impacts of longer-term warming on community structure. This longer-term view is especially important in light of a more recent study exploring the effects of the type, order and temporal spacing of extreme climactic events in rocky intertidal systems (Dal Bello et al. 2017). Dal Bello et al. (2017) found that increasing the temperature of epilithic microphytobenthos (using heated aluminum containers placed over experimental plots for at least six hours) resulted in memory effects in biomass when warming occurred 60 days apart, but not 15 days apart. This finding demonstrates the important role long-term thermal histories may play in intertidal community structure and dynamics, and underlines the importance of capturing long-term data whenever possible.

Heat-budget models enable the prediction or hindcasting of long-term time series of body temperatures from environmental data, time series that would otherwise be difficult if not impossible to obtain. To date, heat-budget models have been developed for four key intertidal species: the red alga Mastocarpus papillatus (Bell 1995), the mussel Mytilus californianus (Helmuth 1998), the limpet Lottia gigantea (Denny and Harley 2006) and the sea star Pisaster ochraceus (Szathmary et al. 2009). These models suggest that body temperatures in algae and mussels that have relatively little contact with the substrate are determined primarily by air temperature, while body temperatures in gastropod grazers and algae that have strong contact with the substrate are determined primarily by substrate temperature. Thus, Bell (1995), Helmuth (1998) and Denny and Harley (2006) have provided the groundwork required to begin to make community-level body temperature predictions.

In this study, we used passively warmed, in situ rock settlement plates in concert with biological surveys and a mechanistic heat-budget model of plate temperature to document for the first time the impact of long-term warming on intertidal communities in central California. As part of an unrelated project (Osborn 2005), settlement plates were deployed in 2002 and mounted atop 1 cm-thick plastic squares. We developed an opportunistic study based on this experimental design, hypothesizing: 1) that the plastic caused the experimental plates to be significantly warmer than the adjacent granite bedrock (the controls) during afternoon low tides; 2) that there would be detectable differences between plate and

bedrock community structure and 3) that the long-term thermal histories of the plates and adjacent bedrock, generated using a mechanistic heat-budget model, would have more power to predict current community structure than recent, short-term measurements.

#### **Methods**

#### **Deployment of settlement plates**

As part of a separate project with different experimental aims (Osborn 2005), settlement plates were deployed in 2002 in the intertidal zone adjacent to Hopkins Marine Station (HMS, 36°62′17″N, 121°90′43″W) in Monterey Bay, California, USA (Fig. 1). Plates were placed between 1.2 and 1.9 m above mean lower low water (MLLW), oriented approximately horizontally, and were composed of four rock types: granite, sandstone, slate and basalt. Each plate was 10 cm long, 10 cm wide and 1 cm thick, and maintained the natural topography of the rock on the settlement surface. Plates were mounted atop 1 cm-thick plastic squares (polyvinyl chloride, PVC) of the same size, and were attached to the granite bedrock via a single, centrally-placed bolt. To facilitate unimpeded movement by motile animals, smooth transitions between the plates and the bedrock were created using Z-spar marine epoxy (A-788 Splash Zone Compound). The twelve plates selected for temperature measurements (Supplementary material Appendix 1 Table A1) were within a 3×2m area, and were arranged in pairs. Three pairs were granite, one sandstone, one basalt and one slate. Plates remained undisturbed between 2002 and the initiation of this experiment in 2013.

#### **Short-term measurements of plate temperature**

To obtain temperature measurements in the field on each experimental plate and its adjacent bedrock control, type-T

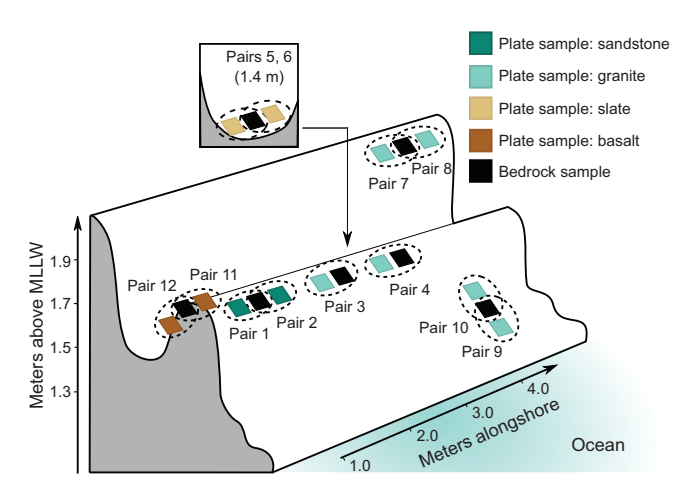


Figure 1. Diagram of field site. Plate samples were paired with bedrock samples; some bedrock samples were shared between two plates. Each plate–bedrock pair is encircled by a black dashed line and labeled.

thermocouples (TT-T-24-SLE, Omega Engineering Inc.) were embedded near the rock surface. A diamond-coated bit was used to create a 2 mm-deep groove in the rock surface, and the thermocouple tip was secured inside it using a small quantity of Z-spar marine epoxy. Thermocouple wires were connected to a multiplexer (AM416, Campbell Scientific) and data logger above the high tide line.

Temperature measurements were acquired once per minute, continuously, from 1 August to 30 September 2013. From these data, we calculated maximum daily temperature and daily degree minutes above threshold (°minutes hereafter) for each experimental plate and its paired bedrock control. °minutes were defined as

°minutes = 
$$\sum_{i=1}^{n} (T_i - T_{\text{th}}) \Delta t$$

where  $T_i$  is the measured temperature at time i within a day,  $\Delta t$  is the time between temperature measurements (1 min), n is 24 h divided by  $\Delta t$ , and  $T_{\rm th}$  is a threshold temperature. The threshold temperature was chosen to be 25°C, the temperature at which many intertidal organisms begin to produce heat stress proteins (Somero 2002). To determine whether the experimental plates were significantly warmer than the bedrock controls, paired t-tests were performed on our time series of maximum daily temperatures and daily °minutes. These analyses were performed in MATLAB R2016b (MathWorks).

### **Biological surveys**

 $30 \times 30$  cm photoquadrats were taken seasonally, in August and December of 2013, and March and June of 2014, centered on each plate. Using the program photoQuad, a  $10 \times 10$  cm quadrat was drawn encompassing the plate, and a stratified random distribution of 50 points was used to estimate the percent cover of sessile taxa. Mobile invertebrates were then counted individually. This procedure was repeated for three, randomly chosen,  $10 \times 10$  cm bedrock plots directly adjacent to each plate.

Organisms were identified to the species level whenever possible. One species commonly found in our survey area, the red alga Mastocarpus papillatus, has a tetrasporophyte life history phase that was long believed to be a separate species (termed Petrocelis) (Guiry et al. 1984). We chose to consider Mastocarpus papillatus and Petrocelis as separate entities due to the possibility that their large morphological differences (foliose as opposed to crustose in form) might drive differences in their response to temperature. In addition, we included two categories intended to capture changes in the percent cover of intertidal epilithic microscopic organisms: red encrusting algae and biofilm. If these organisms were dense enough to be visible to the naked eye, they were grouped according to color (red for red encrusting algae and green for biofilm) to allow for possible differences in response to temperature. Although microscopic organisms are known to coat all hard surfaces submerged in water (Sekar et al. 2004), if they were not dense enough to be visible, the category 'bare rock' was used.

Total percent cover of sessile taxa, sessile richness of taxa and mobile richness of taxa were calculated for each plate and bedrock plot; these metrics were then averaged across the three bedrock plots. To evaluate whether there were quantifiable differences in community structure between plates and the adjacent bedrock, paired t-tests were performed.

#### Mechanistic heat-budget model

A heat-budget model (Denny and Harley 2006), written in MATLAB R2012b (MathWorks), was used to hindcast the thermal histories of the plates and adjacent bedrock using local environmental data and the physical properties of the plates. The model incorporated four mechanisms of heat exchange: short-wave, long-wave, convective and conductive flux. These components were calculated as described by Denny and Harley (2006), with the following adjustments:

- Throughout the model, we assumed that heat transfer occurred only across the top and bottom surfaces of the plates. Thus, in all calculations, a surface area of 100 cm<sup>2</sup> was used.
- 2. The convective heat transfer coefficient,  $h_c$ , was calculated rather than estimated empirically (Denny 2016).
- 3. In solving for temperature, we set the sum of heat fluxes to the change in plate temperature through time multiplied by thermal inertia, rather than to zero, because time dependence could not be ignored.
- 4. The rock plate and underlying layer of PVC were incorporated into the conductive heat transfer calculations.

Adjustments 2–4 are described in detail in the following sections.

#### Calculating the convective heat transfer coefficient

The convective heat transfer coefficient can be defined as

$$h_c = \frac{K \alpha Re^{\beta}}{l_c}$$

where K is the thermal conductivity of air (which ranges from  $0.0247\,\mathrm{W\,m^{-1}}$  K to  $0.0276\,\mathrm{W\,m^{-1}}$  K between  $0^{\circ}\mathrm{C}$  and  $40^{\circ}\mathrm{C}$  respectively), Re is the Reynolds number of the plate in air (calculated as  $l_c$  multiplied by the mainstream velocity [m s<sup>-1</sup>] and divided by the kinematic viscosity of air [m<sup>2</sup> s<sup>-1</sup>]) and  $l_c$  is the characteristic length of the plate or bedrock sample (10 cm) (Denny 2016). Values of  $\alpha$  = 0.593 and  $\beta$  = 0.5 were used (as measured for a flat plate in laminar flow, Denny 2016).

### Solving for temperature with time-dependence

In solving for temperature, Denny and Harley (2006) were able to set the sum of heat fluxes equal to zero because of the rapidity with which limpet body temperatures equilibrate

with environmental temperatures. In our case, however, the rock plates took longer than the model time step (10 min) to reach thermal equilibrium. Thus, time dependence could not be ignored.

As in Denny and Harley (2006), we incorporated conductive heat flux into our model by calculating temperatures at n points along an imaginary vector, T, that descended through the plate and underlying plastic, and into the bedrock below (Fig. 2). Point  $T_{i=1,t}$  represented the temperature at the surface of the plate at time t, and point  $T_{i=n,t}$  was assumed to be equivalent to sea surface temperature at time t. In our case, the distance between points i and i+1 was  $0.001 \, \mathrm{m}$ , n=1021 (corresponding to a depth of 1 m into the bedrock), and the sum of heat fluxes was set equal to  $\Delta T_t$ :

$$\Delta T_t \simeq AT_t$$

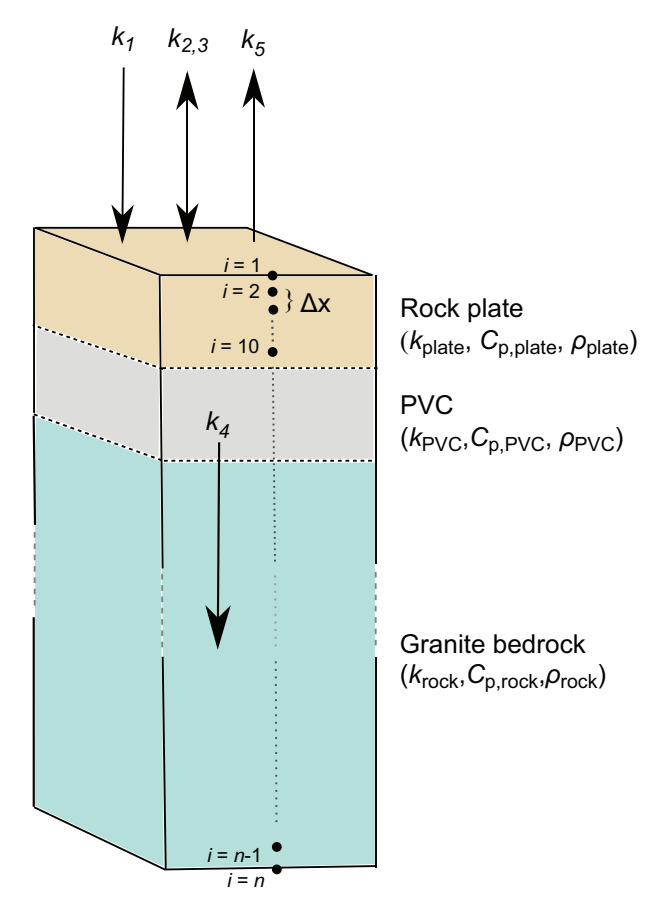


Figure 2. Visualization of heat exchange. Short-wave heat transfer  $(k_1)$ , long-wave heat transfer  $(k_2)$  and  $k_3$  and convective heat exchange  $(k_5)$  affect the temperature at the surface of the rock plate (spatial node i=1). As these factors cause the surface temperature to change, conductive heat transfer  $(k_4)$  occurs through the underlying plate, PVC and granite bedrock, affecting spatial nodes i=2 to i=n. Each layer has unique thermal properties (conductive heat transfer coefficient k, specific heat capacity  $C_p$  and density p) that affect the rate of this process. The spatial resolution between points p and p are the sum of p and p

In this equation, *A* is the following *n* by *n* matrix:

$\left(-a-bk_3-bk_5\right)dt$	adt	0		0	0	$\left(k_1 + k_2 + k_3 T_a + k_5 T_a\right) b dt$
adt	-cdt - adt	cdt	0	•••	0	0
0	adt	-cdt - adt	cdt	0	•••	0
:	··.	··.	٠.	·	··.	:
0			adt	-cdt - adt	cdt	0
0			0	adt	-cdt - adt	cdt
0	0	0	0	0	0	0

where  $k_1$  is short-wave heat transfer,  $k_2$  and  $k_3$  are components of long-wave energy transfer,  $k_5$  is a component of convective heat transfer,  $T_a$  is the temperature of the air at time t, and

$$a = \frac{k_{i,i+1}}{\rho C_p \Delta x^2}; \text{ units} = \left[\frac{1}{s \times kg \times m}\right]$$

$$b = \frac{1}{\rho C_p s^2 \Delta x}; \text{ units} = \left[\frac{K \times s^2}{kg^2 \times m^2}\right]$$

$$c = \frac{k_{i+1,i+2}}{\rho C_p \Delta x^2}; \text{ units} = \left[\frac{1}{s \times kg \times m}\right]$$

where  $k_{i,i+1}$  is the conductive heat transfer coefficient between spatial points i and i+1, which may be part of the plate, PVC plastic or rock layer of the model;  $\rho$  is the mass density of the relevant layer;  $C_p$  is the specific heat capacity of the relevant layer; s is the side length of the plate, 0.1 m; and  $\Delta x$  is the distance between points i and i+1 within the plate, 0.001 m. A finite-difference approach was then employed in solving the following equation:

$$T_{t+1} = T_t + \Delta T_t$$

#### **Incorporating the plate and PVC layers**

The rock plate and underlying layer of PVC were incorporated into the heat-budget model in the conductive heat transfer calculations. Instead of a time step of 30 s and a spatial increment of 1 cm (Denny and Harley 2006), we reduced the spatial increment in the finite-difference approximation of the conductive flux equation to 1 mm to resolve thermal gradients inside the 1-cm-thick layers of rock and PVC. A corresponding reduction in time step to 0.25 s was required to maintain the stability of the calculation.

#### Heat-budget model for bedrock controls

To hindcast the thermal histories of the bedrock control plots, the mechanistic heat-budget model described above was used. However, to predict the temperature of the bedrock's surface, we did not need to account for the rock settlement plate or

PVC layers. Thus, these were excluded when estimating bedrock temperature.

### Parameterizing the heat-budget model

Environmental input data to our heat-budget model included sea surface temperature, air temperature, solar irradiance, wind speed, measured tidal height and significant wave height. Air temperature, solar irradiance and wind speed were obtained from a weather station at HMS using a temperature sensor mounted in a radiation shield (UT12VA), a LI200x and a 5103 propeller anemometer (R. M. Young, Traverse City, MI, USA) mounted 3 m above the ground. The near-substratum velocity was estimated to be 62% of that at 3 m (Denny et al. 2006). Tidal heights were obtained from the NOAA tide gauge at Monterey Harbor (3km from HMS) and significant wave heights were measured using a Datawell Directional buoy positioned approximately 500 m offshore. Sea surface temperatures were available from HMS, where they are taken daily at 08:00 h. These environmental measurements have been consistently available at HMS since 1999.

To populate the physical parameters in the heat-budget model, we relied as much as possible on known quantities. For each plate, tidal height and surface area were measured, while density, specific heat capacity and thermal conductivity were available in the literature ( $\rho_{\text{sandstone}} = 2250 \, \text{kg m}^{-3}$ ,  $C_{p,\text{sandstone}} = 0.92 \, \text{J kg}^{-1}$  K,  $k_{\text{sandstone}} = 1.7 \, \text{W m}^{-1}$  K,  $\rho_{\text{granite}} = 2601 \, \text{kg m}^{-3}$ ,  $C_{p,\text{granite}} = 0.79 \, \text{J kg}^{-1}$  K,  $k_{\text{granite}} = 3.0 \, \text{W m}^{-1}$  K,  $\rho_{\text{basalt}} = 2900 \, \text{kg m}^{-3}$ ,  $C_{p,\text{basalt}} = 0.76 \, \text{J kg}^{-1}$  K,  $k_{\text{slate}} = 2.0 \, \text{W m}^{-1}$  K,  $\rho_{\text{basalt}} = 2900 \, \text{kg m}^{-3}$ ,  $C_{p,\text{basalt}} = 0.84 \, \text{J kg}^{-1}$  K,  $k_{\text{basalt}} = 1.7 \, \text{W m}^{-1}$  K). Infrared emissivity was assumed to be 0.95, a reasonable value for most natural materials (Lyon 1962). Similarly, for the PVC layer, the density, specific heat capacity and thermal conductivity were set to  $\rho_{\text{PVC}} = 1400 \, \text{kg m}^{-2}$ ,  $C_{p,\text{PVC}} = 900 \, \text{J kg}^{-1}$  K and  $k_{\text{PVC}} = 0.16 \, \text{W m}^{-1}$  K, respectively, from published values.

A parameter called 'swash' was incorporated into the model to account for the fact that the plate and bedrock samples were often splashed by waves even when they were above the still-water level of the tide (Denny et al. 2006). After each time step in the model, swash was defined as:

$$Swash = \frac{A_{th} - M_{th}}{w}$$

where  $A_{\rm th}$  is the effective tidal height of the field site,  $M_{\rm th}$  is the tidal height measured by the NOAA tide gauge 3 km from the field site and w is the significant wave height as measured by the buoy 500 m offshore. Swash and short-wave absorptivity were left as variables to be adjusted for model accuracy.

#### Fitting the model and calculating error

The goal of the heat-budget model was to accurately hindcast the daily maximum temperature and daily ominutes experienced by the plates and the adjacent bedrock during the 11 years leading up to our biological measurements. To fit the model to our field data, the model was used to predict these two measures from August to October 2013 for each plate and bedrock sample, and for all combinations of swash and short-wave absorptivity values between 0.5 and 1 with an interval of 0.05. Modeled daily maximum temperatures were plotted against measured daily maximum temperatures, and the slope, intercept and coefficient of determination of the linear regression were calculated. For each plate and bedrock sample, we chose swash and short-wave absorptivity values that maximized the coefficient of determination (R<sup>2</sup>). This process was repeated to select the appropriate swash and short-wave absorptivity values for regressions of modeled versus measured daily ominutes. The final parameters used for each plate and bedrock sample are listed in the Supplementary material Appendix 1 Table A2.

Once final swash and short-wave absorptivity values were determined, the accuracy of the relevant linear regression was used to calculate an error estimate for modeled daily maximum temperature and daily °minutes. We bootstrapped the residuals of the linear fits over 1000 iterations to provide 95% confidence intervals for both temperature measures (Supplementary material Appendix 1 Table A2). We also performed paired t-tests to determine the success of model fitting to field data; these tests compared the maximum daily temperatures and daily °minutes measured empirically between 1 August and 30 September 2013 for each plate and bedrock sample with those computed by the heat-budget model for each sample over the same time period.

#### **Generating hindcasts**

Once best-fit parameters and 95% confidence intervals had been determined for each plate and bedrock sample, the heat-budget model was used in concert with historical environmental data from HMS to generate thermal time series for each plate and bedrock sample from January 2002 to October 2013, the period over which the plates were deployed. For each sample, a time series optimized for calculating maximum daily temperature and a time series optimized for calculating daily °minutes were produced, using the best-fit parameters associated with each measure. Environmental records during this time period were linearly interpolated to every ten minutes to match model output.

Maximum daily temperature and daily °minutes were calculated for all time series and adjusted using the best-fit regression

lines between measured and modeled values. For each value, we used the intercept and slope of the regression to transform the data such that the intercept became 0 and the slope became 1. That is, we subtracted the intercept and divided by the slope. We then calculated significant annual temperature  $S_T$  and significant annual  $^{\circ}$ minutes  $S_D$ . Significant annual temperature during year i,  $S_{TP}$  was the maximum daily temperature over the 10 warmest days of summer, averaged. Similarly, significant annual °minutes during year i,  $S_{D,i}$ , was the daily °minutes of the 10 warmest days of summer, averaged. Average significant annual temperature and average significant annual °minutes were obtained by taking the mean of  $S_{Ti}$  and  $S_{Di}$  between 2002 and 2013. To examine differences between significant annual temperatures and significant annual ominutes on the plate samples relative to the bedrock samples between 2002 and 2013, we performed paired t-tests.

# Long-term effects of temperature on community structure

We employed three statistical techniques to explore potential links between current community structure and long-term warming. First, we analyzed our community-level biological data using PRIMER ver. 6. MDS plots based on Bray-Curtis similarities were used to visualize differences in structure between plate and bedrock communities across seasonal surveys and temperature treatments. Analysis of similarity (ANOSIM) was used to test for differences in community structure due to season. Finding that season did not result in significantly different community structures, we averaged the percent cover, sessile richness of taxa and mobile richness of taxa of each plate and bedrock sample across seasons, and used ANOSIM to test for differences due to temperature treatment (Clarke and Warwick 2001). Top contributors to these differences in community composition were identified using a similarity percentage test (SIMPER) (Clarke and Warwick 2001).

Second, we used the following linear regression model:

$$(y_{\text{bedrock}} - y_{\text{plate}}) \sim (\overline{S_{T,\text{plate}}} - \overline{S_{T,\text{bedrock}}}) \times \text{season}$$

In this equation, y is mobile richness of taxa, sessile richness of taxa or percent cover of sessile taxa, and  $S_T$  is average significant annual temperature. We expected that increased differences in average significant annual temperatures between plate and bedrock pairs would correlate with increased differences in richness of taxa and percent cover.

Third, a recently developed multivariate Bayesian approach (Clark et al. 2017) allowed us to incorporate our mobile and sessile taxa data into a single, supplementary analysis examining the community-level effects of temperature. Generalized joint attribute modeling, or GJAM, allows for such joint analysis of diverse community-level data types while still taking into account the effects of multiple environmental covariates. We used GJAM to 1) incorporate both percent cover of sessile taxa and counts of mobile taxa in the same analysis, 2)

evaluate which common intertidal species (i.e. those observed at least once on both the plate and bedrock samples) were significantly affected by temperature and tidal height and 3) use the resulting model to predict how the abundance of specific organisms at different tidal heights might shift in response to substrate warming of 2°C. Plate–bedrock pair number was included as a random factor in the model, and the deviance information criterion (DIC) was used to select the best set of predictor variables (Clark et al. 2017). The model was fitted using non-informative priors, 100 000 iterations with a burnin of 30 000, and the R package gjam (Clark et al. 2017).

# Comparing the power of short-term and long-term temperature data

Finally, we endeavored to explore whether long-term thermal histories had more power to predict current community structure than recent, short-term measurements. To do this, we used the following linear regression model:

$$BC_{plate, bedrock} \sim (x_{plate} - x_{bedrock})$$

In this equation, BC is the Bray–Curtis similarity between a plate and the adjacent bedrock, and x is a temperature metric. We hypothesized that plate–bedrock pairs that experienced larger temperature differences would have smaller Bray–Curtis similarities. We used the strength of the linear regression (as measured by the coefficient of determination,  $R^2$ ) as a proxy for predictive power.

Using this framework, we conducted two tests. First, we explored to what extent each individual year of data (i.e.  $S_{T,i}$  where i ranged between 2002 and 2013) could predict current community structure. As part of this analysis, we also tested to what extent average daily maximum temperature, as measured on our plates and bedrock controls in the field in 2013, could predict current community structure. Second, we explored predictive power cumulatively through time. For example, we initially defined x as  $S_{T,2013}$  and obtained  $R^2$ . Then, we added years sequentially to average significant annual temperature (i.e.  $x = \overline{S_{T,2012-2013}}$ ,  $x = \overline{S_{T,2011-2013}}$ , etc.). We observed whether  $R^2$  generally increased or decreased as more years were considered.

#### Results

#### Measured temperature data

In the field, average daily maximum temperatures on the experimental plates were found to be significantly higher than those on the adjacent bedrock controls ( $t_{11}$ =5.8, p<0.001) (Supplementary material Appendix 1 Table A3). The temperature treatment resulted in an average increase of  $2.7\pm0.5^{\circ}$ C relative to the bedrock. Similarly, daily °minutes on the plates were significantly higher than those on the adjacent bedrock ( $t_{11}$ =6.9, p<0.001) (Supplementary material

Appendix 1 Table A3). Due to the temperature treatment, the plates experienced an average of  $362.5 \pm 52.7$  additional °minutes per day relative to the bedrock.

Although plate–bedrock pairs ranged from 1.3 to 1.9 m above MLLW in tidal height, temperature differences within plate–bedrock pairs were not correlated with tidal height (R=0.03, p=0.92). The rock type of the plates likely contributed to differences in temperature and  $^{\circ}$ minutes between plate and bedrock pairs (Supplementary material Appendix 1 Fig. A1), but because our plates were deployed by a separate research team to address a separate set of hypotheses 12 years before the initiation of our experiment, there was insufficient replication of rock types to explore these effects statistically.

#### **Current community structure**

Biological surveys yielded observations of 14 sessile and 7 mobile taxa, including barnacles from the genera *Balanus* and *Chthamalus*, algae from the genera *Endocladia* and *Mastocarpus*, mussels (*Mytilus californianus*), and limpets from the genus *Lottia*. Paired t tests indicated that individual plate communities had  $1.61 \pm 0.26$  fewer sessile taxa than did the adjacent bedrock, averaged across seasons (Supplementary material Appendix 1 Table A4). Similarly, plate communities had  $0.55 \pm 0.22$  fewer mobile taxa and  $13.8 \pm 5.5\%$  lower cover of sessile taxa than the adjacent bedrock.

#### Hindcasted temperature data

Between 2002 and 2013, significant annual temperatures on the experimental plates were significantly higher than those on the adjacent bedrock controls ( $t_{11}$ =4.3, p=0.001) (Fig. 3). The temperature treatment resulted in, on average, a hindcasted increase of  $2.8\pm0.7^{\circ}\text{C}$  relative to the bedrock. Similarly, significant annual °minutes on the plates were significantly higher than those on the adjacent bedrock ( $t_{11}$ =4.9, p<0.001). Due to the temperature treatment, the plates experienced an average of  $1173.6\pm237.9$  additional significant annual °minutes relative to the bedrock.

## Accuracy of hindcasts

Our mechanistic heat-budget model tended to slightly underpredict measured daily maximum temperature, and slightly over-predict measured daily °minutes. Hindcasted maximum daily temperatures for 1 August through 30 September 2013 were an average of 1.1±0.1°C lower than those measured in the field for all plate–bedrock pairs (Supplementary material Appendix 1 Table A5); hindcasted daily °minutes for the same time period were 88.4±20.3 °minutes higher than those measured in the field for all plate–bedrock pairs (Supplementary material Appendix 1 Table A5).

When considering the entire 12 years of hindcast temperatures, for both temperature and °minutes, significant annual values were consistently higher than the average maximum daily values observed in the field in 2013. This trend is due to higher hindcasted temperatures for both plate and bedrock

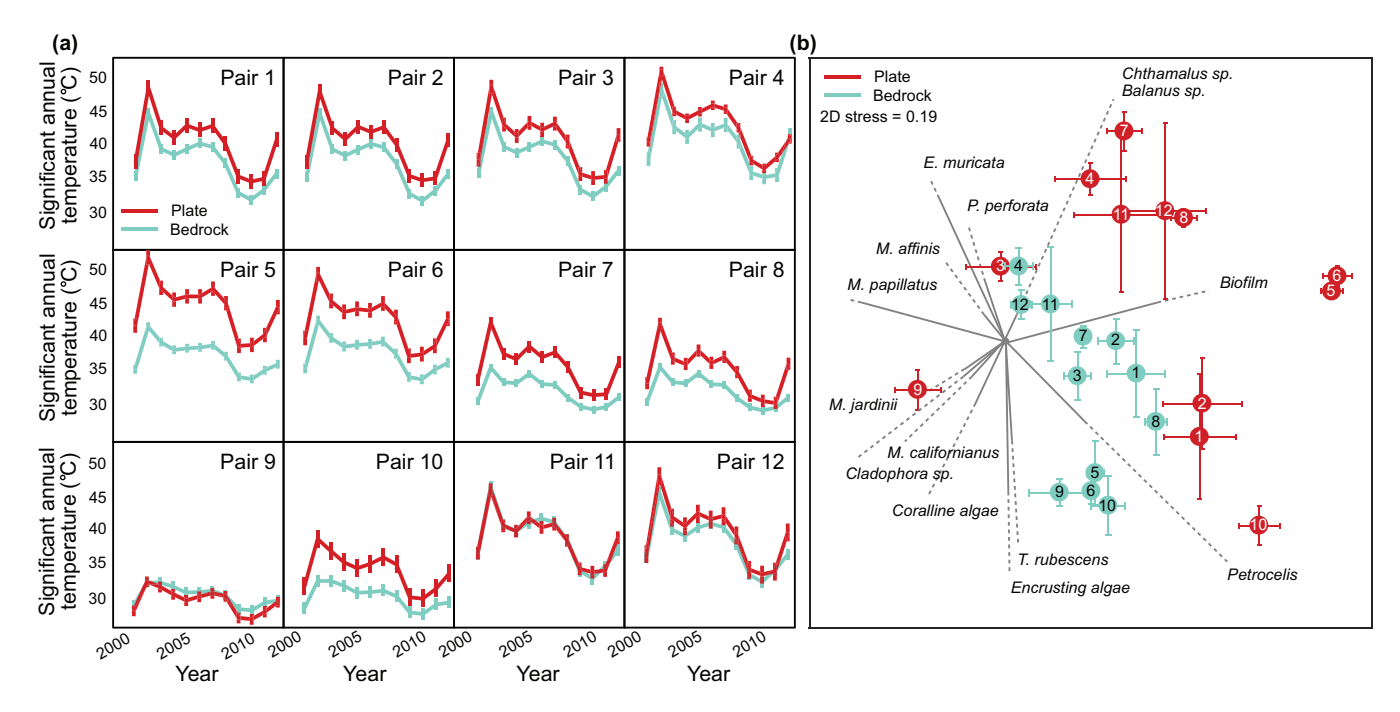


Figure 3. Experimentally-warmed plate communities had significantly different composition than the bedrock controls. (a) Hindcasted temperatures for plate–bedrock pairs; error bars represent 95% confidence intervals. (b) MDS plot of plate and bedrock communities; points indicate the average location ± standard error after averaging across seasons, and are labeled by pair number. Length and labels of vectors indicate the relative contributions of taxa to community-level differences.

samples during the first six years of the study, between 2002 and 2008 (Fig. 3). These warmer hindcasted temperatures are consistent with local air temperature data for 2002–2008. Note that recent, cooler years are part of a longer warming trend (Supplementary material Appendix 1 Fig. A2).

#### Effects of temperature on community structure

Analysis of similarity indicated that communities did not vary significantly by season (R = -0.01, p = 0.64). However, the temperature treatment did have a statistically significant effect on community composition (R = 0.25, p = 0.001) (Fig. 3). Plate communities exhibited reductions in algae, barnacles, mussels and other common intertidal taxa. They were characterized primarily by biofilm (26.5%), the red algae *Endocladia muricata* (14.3%) and red encrusting algae (10.3%), while the bedrock communities were primarily characterized by red encrusting algae (26.9%), *E. muricata* (14.7%) and the red algae *Mastocarpus papillatus* (14.1%).

Differences in mobile and sessile richness of taxa were positively related to differences in temperature ( $F_{1,40}$ =7.7, p=0.008 and  $F_{1,40}$ =10.74, p=0.002 respectively). Season was not a significant factor in these analyses ( $F_{3,40}$ =1.46, p=0.24 and  $F_{3,40}$ =1.27, p=0.30 respectively), and did not interact significantly with temperature ( $F_{3,40}$ =0.54, p=0.66 and  $F_{3,40}$ =1.4, p=0.26 respectively). Differences in percent cover were not related to differences in temperature ( $F_{1,40}$ =0.13, p=0.72), but were significantly related to season ( $F_{3,40}$ =4.41, p=0.01) with percent cover being higher in December 2013 and June 2014 than during the other seasons.

GJAM indicated that temperature, tidal height and the interaction between temperature and tidal height all significantly affected species abundance. Temperature had a negative effect on the abundance of T. rubescens, M. papillatus, Petrocelis, Lottia sp. and other mobile taxa, while it had a positive effect on rock and biofilm (Supplementary material Appendix 1 Fig. A4). Biofilm and *T. rubescens* decreased with tidal height, while Littorina sp., M. papillatus, Endocladia muricata and rock increased with tidal height. Finally, the interaction between temperature and tidal height had a negative effect on biofilm abundance, but a positive effect on the abundance of rock, M. papillatus and other sessile taxa. As a result, the percent cover of biofilm increased with temperature at lower tidal heights, but decreased with temperature at higher tidal heights. Conversely, the percent cover of rock, M. papillatus and other sessile taxa decreased with temperature at lower tidal heights, but increased with temperature higher tidal heights.

These outcomes are illustrated as boxplots in Supplementary material Appendix 1 Fig. A4 and as heatmaps in Supplementary material Appendix 1 Fig. A5. Supplementary material Appendix 1 Figure A5 also displays covariance matrices, in which the residual co-dependence among species is shown after the main model structure explained by temperature, tidal height and their interaction is removed. Clustering analysis detected two groups of species that tended to covary. The first group contained red encrusting algae, *Lottia* sp., *Littorina* sp., *M. papillatus*, encrusting coralline algae, *Cladophora sp.*, articulated coralline algae, *T. rubescens*, *Petrocelis*, other sessile taxa, other mobile taxa and

rock where barnacles had been ripped off the substrate. This group was correlated with lower temperatures and lower tidal heights. The second group contained *Endocladia muricata*, rock, barnacles, *P. perforata* and biofilm, and was correlated with higher temperatures and higher tidal heights.

To better visualize species-specific responses to temperature and tidal height, we used the model to predict changes in the abundance of eight species as temperature increased from 24 to 26°C at 1.0 m above MLLW and from 30 to 32°C at 2.0 m above MLLW (Supplementary material Appendix 1 Fig. A6). The species selected were those identified to be significantly affected by temperature: T. rubescens, M. papillatus, Petrocelis, Lottia sp., other mobile taxa, rock and biofilm. Initial temperatures of 24 and 30°C were chosen because they are representative of current bedrock temperatures during summer afternoon low tides; an addition of 2°C was chosen due to its relevance in a near-future climate change scenario. At 1.0 m above MLLW, biofilm, Petrocelis and T. rubescens are expected to increase with increasing temperature, while at 2.0 m above MLLW, M. papillatus, rock and other sessile taxa are expected to increase.

# Predictive power of short- and long-term temperature measurements

First, we defined x as average daily maximum temperature (as measured in the field in 2013). There was no significant relationship between the structure of plate and bedrock communities and differences in these short-term, measured temperatures ( $F_{1,10}$ =0.46, p=0.51,  $R^2$ =0.04) (Fig. 4a). Next, we defined x as average significant annual temperature (as hind-casted by our heat-budget model), and found a significant relationship between the structure of the plate and bedrock communities and differences in these long-term, hindcasted temperatures ( $F_{1,10}$ =5.88, p=0.04,  $R^2$ =0.37) (Fig. 4a). The strength of this relationship (as measured by  $R^2$ ), increased as additional significant annual temperature differences

were included sequentially in the average (Fig. 4b). Finally, we found that  $R^2$  tended to be larger for years during which significant annual plate temperature was higher ( $F_{1,10} = 1.45$ , p = 0.26,  $R^2 = 0.13$ ) (Fig. 4c).

#### Discussion

Our long-term, in situ warming experiment explores how intertidal communities may change over the coming century, and suggests that these changes may be cumulative over years of exposure. The inclusion of an insulating PVC layer between our rock settlement plates and the granite bedrock increased the average maximum daily temperature experienced by organisms on the plates by about 2.7°C from 2002 to 2013. This temperature increase is commensurate with moderate shifts in air temperature predicted to occur by 2100 (Pachauri and Meyer 2014). Our data suggest that this temperature increase will result in decreases in richness of taxa and in the percent cover of filamentous algae, barnacles, mussels and mobile grazers. Only the percent cover of biofilm is likely to increase. Importantly, our study also demonstrates that heat-budget models are powerful tools that can reveal the thermal histories of organisms and communities, and that modern communities reflect their thermal histories. Using 12 years of hindcasted data, we were able to double our ability to predict current community structure from the increased temperature of the plates and show that warm years in the relatively distant past may be more predictive of current community structure than recent, cooler years.

# Effects of long-term warming on community structure

Our results suggest that short-term measurements of differences between plate and bedrock temperatures were not sufficient to predict differences in community structure. However, long-term differences in average significant annual

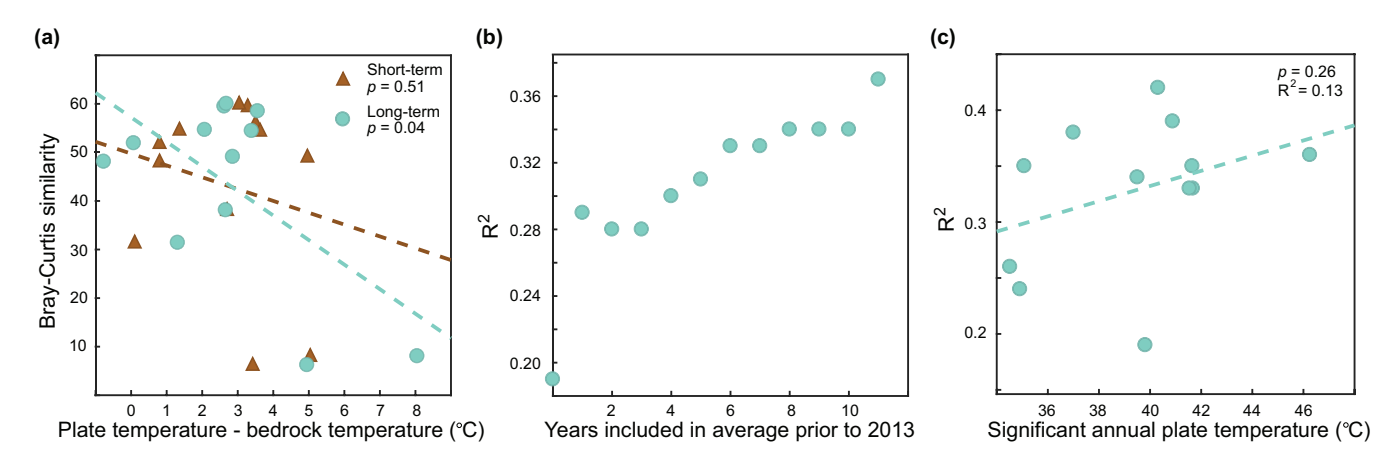


Figure 4. Long-term hindcasts predicted modern community structure. (a) Differences in temperature between plate–bedrock pairs were negatively related to their Bray–Curtis similarity. Linear regressions are shown in dashed lines. (b) Differences in average significant annual temperature explained more of the variation in Bray–Curtis similarity as temperature data from more years prior to 2013 were subsequently included in the average. (c)  $R^2$  values tended to be higher during warmer years.

temperatures did so, indicating that the current communities we observed were not determined by just contemporary temperatures; instead, these communities reflected their 12-year thermal histories. In addition, our approach revealed that not all years had equal power to account for the structure of modern communities.

It is possible that these observations might have been confounded by other factors that can drive differences in intertidal community structure, such as wave exposure, recruitment, succession and species interactions. However, to minimize the possible influences of wave exposure and recruitment, we analyzed our data in plate–bedrock pairs with each plate located within 10 cm of its bedrock control. Although reproductive output and larval survival, and oceanic conditions that affect larval supply (including upwelling and wave intensity), are expected to change as sea surface temperatures increase (Bakun 1990, Helmuth et al. 2006b, Zacharioudaki et al. 2011), our experimental design assumed that variation in these unmeasured factors would be minimized on the sub-10 cm scale.

Succession might also have influenced the structure of the plate and bedrock communities. However, plots adjacent to the plates that were cleared at the time of deployment in 2002 (Osborn 2005) were visually indistinguishable from the bedrock communities in 2013, and could not be located. In addition, previous intertidal succession studies had recovery times ranging from 6 months to >37 months (Hewatt 1935, Northcraft 1948, Glynn 1965), suggesting that our plate communities, without the temperature treatment applied, would have been statistically indistinguishable from the adjacent bedrock within the first 3–4 years of our study.

Last, it is worth noting that temperature can indirectly affect community structure through species interactions. For example, Kordas et al. (2017) observed that the presence of limpet grazers attenuated the effects of warming on the trophic structure of intertidal communities, and Poloczanska et al. (2008) found that the dominant competitor between two intertidal barnacle species shifted under warming conditions (Poloczanska et al. 2008, Kordas et al. 2017). Shifts in competition, predation and facilitation may have influenced the effects of temperature on the intertidal communities on our experimental plates.

#### Changes in community composition

Observed differences between plate and bedrock communities were likely driven by the thermal ecology of common intertidal species. Encrusting microbial films (classified as biofilm or red encrusting algae in this study) consist primarily of diatoms, cyanobacteria and macroalgal germlings, and to our knowledge, their temperature tolerance is unknown. It is likely that the observed increases in the percent cover of biofilm on our experimental plates resulted in part from decreases in the percent cover of grazers and competitors. Similar increases in encrusting red algae were not observed, however, and further work is required to determine whether and why encrusting red algae might have lower

thermal tolerances than biofilm. Barnacles, red macroalgae and mussels likely have lower temperature tolerances than microbial films (Southward 1958, Bell 1993, Mislan et al. 2014, Gilman et al. 2015). Because of high average significant annual temperatures, we would expect these organisms to survive only on our coolest plates, and this was indeed observed (Supplementary material Appendix 1 Fig. A3).

Our observations generally support those obtained by Kordas et al. (2015). In particular, they also observed a decline in richness of taxa due to decreases in mobile grazers and barnacles when substrate temperatures were increased by about 2°C. However, while we recorded reductions in filamentous algae, Kordas et al. did not. It is possible that this difference was driven by the relatively short duration of their study (1 year), by the relatively low substrate temperatures achieved by their settlement plates even at the highest tidal height tested (29.3°C at 2.6 m above the Canadian chart datum), or by differences in the algal species considered. While these studies represent promising first steps, a concerted effort to deploy and monitor passively heated settlement plates (such as those described here or those used by Kordas et al.) across a latitudinal gradient would do much to strengthen our understanding of the scale, patchiness and strength of climate change effects on intertidal communities.

#### Possible effects of substratum type

There is some evidence that the chemical properties and microtopography of the substratum can influence recruitment, settlement and survival of intertidal organisms (Davis 2009). Our sandstone, basalt and slate settlement plates were less rugose than the granite bedrock to which they were compared, and for these plate-bedrock pairs, substratum type may have contributed to differences in community structure. Prior work has suggested that larvae generally prefer to settle on more rugose surfaces, but that temperature and waveexposure tend to be more influential drivers of community structure than microtopography (Mcquaid and Branch 1984, Davis 2009). Additionally, our granite plates, whose chemical composition and microtopography were consistent with the granite bedrock, showed similar differences in temperature, percent cover and richness of taxa relative to the adjacent bedrock as our non-granite plates. Further investigation using specifically designed and better replicated experiments is required to tease out the relative contributions of rock composition and microtopography to recruitment, settlement and survival.

#### Usefulness of heat-budget models

Heat budget models have traditionally been used to generate long-term time series of individual body temperatures that would be very difficult, if not impossible, to gather using other techniques (Helmuth 1998, Denny and Harley 2006, Denny et al. 2006). Here, we show they can also be used to hindcast temperatures experienced by entire communities, albeit with some limitations. First, our model requires

plentiful, site-specific environmental data. Additionally, changes in substrate temperature do not necessarily translate to changes in body temperature across all functional groups of intertidal organisms. Gastropod grazers and filamentous and encrusting algae tend to have body temperatures that are very close to the substrate temperature (Denny and Harley 2006); these organisms were the most common at our study site. However, erect algae and mussels, which have only small proportions of their surface area in contact with the substrate, may have body temperatures controlled more by insolation, convection and evaporation than by conduction (Helmuth 1998, Kordas et al. 2015). Finally, like most models, our heat-budget model can be sensitive to small changes in input parameters, and one must conduct thorough testing and ensure outputs are reasonable if the model is to be useful.

In summary, we used a long-term, in situ experimental approach to determine the effects of climate warming on intertidal communities. A warming treatment of about 2.7°C on our settlement plates over 12 years resulted in community-level shifts toward lower richness of taxa, and lower percent cover of most major groups of intertidal species. Last, we demonstrated that long-term temperature data can be essential to demonstrating significant links between temperature and changes in community structure.

#### Data availability statement

Data are available from the Dryad Digital Repository: <a href="http://dx.doi.org/10.5061/dryad.jwstqjq6k">http://dx.doi.org/10.5061/dryad.jwstqjq6k</a> (LaScala-Gruenewald et al. 2020).

Acknowledgements – We thank D. Osborn for the deployment of plates in 2002, M. Freeman and L. P. Miller for field assistance, J. S. Clark for advice on GJAM implementation and C. D. G. Harley for advice on the manuscript.

Funding – This work was funded by NSF OCE 1130095 and IOS 1655529.

Author contributions – DELG was the primary contributor to the investigation, formal analysis and original draft preparation for this manuscript. MWD acquired the necessary funding. In all other respects, DELG and MWD contributed equally.

#### References

- Bakun, A. 1990. Global climate change and intensification of coastal ocean upwelling. Science 247: 198–201.
- Barry, J. P. et al. 1995. Climate-related, long-term faunal changes in a california rocky intertidal community. Science 267: 672–675.
- Bell, E. 1993. Photosynthetic response to temperature and desiccation of the intertidal alga *Mastocarpus papillatus*. Mar. Biol. 117: 337–346.
- Bell, E. 1995. Environmental and morphological influences on thallus temperature and desiccation of the intertidal alga *Mastocarpus papillatus* Kützing. J. Exp. Mar. Biol. Ecol. 191: 29–55.
- Bertness, M. D. et al. 1999. Climate-driven interactions among rocky intertidal organisms caught between a rock and a hot place. Oecologia 120: 446–450.

- Blenckner, T. et al. 2007. Large-scale climatic signatures in lakes across Europe: a meta-analysis. Global Change Biol. 13: 1314–1326.
- Clark, J. S. et al. 2017. Generalized joint attribute modeling for biodiversity analysis: median-zero, multivariate, multifarious data. – Ecol. Monogr. 87: 34–56.
- Clarke, K. R. and Warwick, R. M. 2001. Change in marine communities: an approach to statistical analysis and interpretation, 2nd edn. Primer-E Ltd.
- Dal Bello, M. et al. 2017. Legacy effects and memory loss: how contingencies moderate the response of rocky intertidal biofilms to present and past extreme events. – Global Change Biol. 23: 3259–3268.
- Davenport, J. and Davenport, J. L. 2005. Effects of shore height, wave exposure and geographical distance on thermal niche width of intertidal fauna. Mar. Ecol. Prog. Ser. 292: 41–50.
- Davis, A. R. 2009. The role of mineral, living and artificial substrata in the development of subtidal assemblages. – In: Wahl, M. (ed.), Marine hard bottom communities. Ecological studies (analysis and synthesis), Vol. 206. Springer.
- Davis, A. J. et al. 1998. Making mistakes when predicting shifts in species range in response to global warming. – Nature 391: 783–787.
- Denny, M. W. 2016. Ecological mechanics: principles of life's physical interactions. Princeton Univ. Press.
- Denny, M. W. and Harley, C. D. G. 2006. Hot limpets: predicting body temperature in a conductance-mediated thermal system. J. Exp. Biol. 209: 2409–2419.
- Denny, M. W. et al. 2006. Thermal stress on intertidal limpets: long-term hindcasts and lethal limits. J. Exp. Biol. 209: 2420–2431.
- Denny, M. W. et al. 2009. On the prediction of extreme ecological events. Ecol. Monogr. 79: 397–421.
- Fields, P. A. et al. 1993. Effects of expected climate change on marine faunas. Trends Ecol. Evol. 8: 361–367.
- Gardner, J. L. et al. 2011. Declining body size: a third universal response to warming? Trends Ecol. Evol. 26: 285–291.
- Gilman, S. et al. 2015. Body temperatures of an intertidal barnacle and two whelk predators in relation to shore height, solar aspect and microhabitat. Mar. Ecol. Prog. Ser. 536: 77–88.
- Glynn, P. W. 1965. Community composition, structure and interrelationships in the marine intertidal *Endocladia muricata – Balanus glandula* association in Monterey Bay, California. – Beaufortia 12: 1–198.
- Graham, R. W. and Grimm, E. C. 1990. Effects of global climate change on the patterns of terrestrial biological communities. Trends Ecol. Evol. 5: 289–292.
- Gruner, D. S. et al. 2017. Effects of experimental warming on biodiversity depend on ecosystem type and local species composition. – Oikos 126: 8–17.
- Guiry, M. D. et al. 1984. Reinstatement of the Genus Mastocarpus Kutzing (Rhodophyta). – Taxon 33: 53–63.
- Harley, C. D. G. 2011. Climate change, keystone predation and biodiversity loss. Science 334: 1124–1127.
- Harley, C. D. G. et al. 2006. The impacts of climate change in coastal marine systems. Ecol. Lett. 9: 228–241.
- Hawkins, S. J. et al. 2008. Complex interactions in a rapidly changing world: responses of rocky shore communities to recent climate change. Clim. Res. 37: 123–133.
- Helmuth, B. 1998. Intertidal mussel microclimates: predicting the body temperature of a sessile invertebrate. Ecol. Monogr. 68: 51–74.

- Helmuth, B. et al. 2002. Climate change and latitudinal patterns of intertidal thermal stress. Science 298: 1015–1017.
- Helmuth, B. et al. 2006a. Mosaic patterns of stress in the rocky intertidal zone: implications for climate change. Ecol. Monogr. 76: 461–479.
- Helmuth, B. et al. 2006b. Living on the edge of two changing worlds: forecasting the responses of rocky intertidal ecosystems to climate change. Annu. Rev. Ecol. Evol. Syst. 37: 373–404.
- Hewatt, W. G. 1935. Ecological succession in the mytilus californianus habitat as observed in Monterey Bay, California. Ecology 16: 244–251.
- Hofmann, G. E. and Somero, G. N. 1995. Evidence for protein damage at environmental temperatures: seasonal changes in levels of ubiquitin conjugates and hsp70 in the intertidal mussel *Mytilus trossulus*. – J. Exp. Biol. 198: 1509–1518.
- Kennett, J. P. and Stott, L. D. 1991. Abrupt deep-sea warming, paleoceanographic changes and benthic extinctions at the end of the Palaeocene. – Nature 353: 225–228.
- Kordas, R. L. et al. 2015. Intertidal community responses to field-based experimental warming. Oikos 124: 888–898.
- Kordas, R. L. et al. 2017. Herbivory enables marine communities to resist warming. Sci. Adv. 3: e1701349.
- LaScala-Gruenewald, D. E. et al. 2020. Data from: Long-term mechanistic hindcasts predict the structure of experimentally-warmed intertidal communities. Dryad Digital Repository, <a href="http://dx.doi.org/10.5061/dryad.jwstqjq6k">http://dx.doi.org/10.5061/dryad.jwstqjq6k</a>.
- Lyon, R. J. P. 1962. Minerals in the infrared: a critical bibliography.
   Stanford Res. Inst. Publ., pp. 76.
- Mcquaid, C. D. and Branch, G. 1984. Influence of sea temperature, substratum and wave exposure on rocky intertidal communities: an analysis of faunal and floral biomass. Mar. Ecol. Prog. Ser. 19: 145–151.
- Mislan, K. A. S. et al. 2014. Geographical variation in climatic sensitivity of intertidal mussel zonation. Global Ecol. Biogeogr. 23: 744–756.
- Northcraft, R. D. 1948. Marine algal colonization on the Monterey Peninsula, California. Am. J. Bot. 35: 396–404.
- Osborn, D. 2005. Rocky intertidal community structure on different substrates. PhD thesis, Univ. of California at Santa Cruz.
- Pachauri, R. K. and Meyer, L. A. 2014. IPCC, 2014: Climate change 2014: sythesis report. In: Contribution of working

Supplementary material (available online as Appendix oik-07468 at <www.oikosjournal.org/appendix/oik-7468>). Appendix 1.

- groups I, II and III to the fifth assessment report of the intergovernmental panel on climate change. IPCC, Geneva.
- Parmesan, C. 2006. Ecological and evolutionary responses to recent climate change. – Annu. Rev. Ecol. Evol. Syst. 37: 637–669.
- Parmesan, C. and Yohe, G. 2003. A globally coherent fingerprint of climate change impacts across natural systems. Nature 421: 37–42.
- Poloczanska, E. S. et al. 2008. Modeling the response of populations of competing species to climate change. Ecology 89: 3138–3149.
- Sagarin, R. D. et al. 1999. Climate-related change in an intertidal community of short and long time scales. Ecol. Monogr. 69: 465–490.
- Sanford, E. 1999. Regulation of keystone predation by small changes in ocean temperature. Science 283: 2095–2097.
- Schiel, D. R. et al. 2004. Ten years of induced ocean warming causes comprehensive changes in marine benthic communities. Ecology 85: 1833–1839.
- Sekar, R. et al. 2004. Laboratory studies on adhesion of microalgae to hard substrates. Hydrobiologia 512: 109–116.
- Shaver, G. R. et al. 2000. Global warming and terrestrial ecosystems: a conceptual framework for analysis. Bioscience 50: 871–882.
- Sheridan, J. A. and Bickford, D. 2011. Shrinking body size as an ecological response to climate change. – Nat. Clim. Change 1: 401–406.
- Somero, G. 2002. Thermal physiology and vertical zonation of intertidal animals: optima, limits and costs of living. – Integr. Comp. Biol. 42: 780–789.
- Southward, A. J. 1958. Note on the temperature tolerances of some intertidal animals in relation to environmental temperatures. J. Mar. Biol. Assoc. 3: 49–66.
- Szathmary, P. L. et al. 2009. Climate change in the rocky intertidal zone: predicting and measuring the body temperature of a keystone predator. Mar. Ecol. Prog. Ser. 374: 43–56.
- Thompson, R. C. et al. 2002. Rocky intertidal communities: past environmental changes, present status and predictions for the next 25 years. Environ. Conserv. 29: 168–191.
- Zacharioudaki, A. et al. 2011. Future wave climate over the west-European shelf seas. Ocean Dyn. 61: 807–827.